# EFFECT OF ELECTRODEPOSITION TEMPERATURE ON CORROSION RESISTANCE OF CALCIUM PHOSPHATE

*Filip Pastorek[1)*], Branislav Hadzima[1, 2)], Miroslav Omasta[1)], Mansour Mhaede[3, 4)]*
*[1)] University of Žilina, Faculty of Mechanical Engineering, Žilina, Slovakia*
*[2)] Research center of the University of Žilina, Žilina, Slovakia*
*[3)] Institute of Materials Science and Engineering, Clausthal University of Technology, Agricolastrasse 6, 38678 Clausthal-Zellerfeld, Germany.*
*[4)] Faculty of Engineering, Zagazig University, Egypt*

Received: 11.10.2013
Accepted: 14.01.2014

*[*]Corresponding author:Filip Pastorek,E-mail address: filip.pastorek@fstroj.uniza.sk, Tel.: +421 949 413 536, Department of Materials Engineering, Faculty of Mechanical Engineering, University of Žilina, Univerzitná 1, 010 26 Žilina,, Slovakia*

**Abstract**
Electrodeposition process of calcium phosphate (CaP) was performed at various temperatures on AZ31 magnesium alloy and the influence on corrosion resistance of the alloy covered by CaP was investigated by electrochemical tests supported by photodocumentation. The electrodeposition treatment was performed by potential controlled method in water solution of $Ca(NO_3)_2.4H_2O$, $NH_4H_2PO_4$ and $H_2O_2$. The difference in the process of CaP formation at various temperatures was described using diagrams of current density time dependence. Corrosion measurements were performed in 0.9% NaCl solution at 22 ± 2 °C using electrochemical impedance spectroscopy. According to corrosion resistance results, the optimal temperature for CaP electrodeposition process was chosen.

**Keywords:** Calcium phosphate; Magnesium alloy; Electrochemical impedance spectroscopy; Light microscopy; Electrodeposition

## 1 Introduction

Commonly used materials for fixing bone fracture are medical-grade metals such as 316L stainless steel, pure titanium and its alloys, and cobalt–chromium-based alloys [1]. If the implant carries too large a component of the applied load, the bone beneath it will experience a reduced load and will lose density in response [2]. The properties of these conventional metallic implants do not match well with bone due to the basic difference in the modulus of elasticity of the two (for cortical bone, in the order of 3–20 GPa, which is an order of magnitude less than that of metals). In case of metal implants, risk of stress shielding of the bone is much higher since a greater portion of the load is on the metallic implants. This stress shielding obstructs the stabilization of the bone tissue and hence multiple surgeries need to be performed, leading to further complications [1, 3-5].

Magnesium has been suggested as a revolutionary implant material to overcome the limitations of the current metallic materials being used. Mg is light in weight and low in density, and exhibits high strength/weight ratio [6]. The elastic modulus of Mg has been reported as 45 GPa[7] and therefore, in comparison with the current metals in clinical use, is far closer to the

DOI 10.12776/ams.v20i2.290 p-ISSN 1335-1532
e-ISSN 1338-1156

elastic modulus of bone. Current magnesium alloys exhibit good mechanical and fatigue properties [8, 9]. Mg also has the advantage of degradation, and thus if corrosion rates are controlled, the material would slowly degrade, removing the necessity for second removal surgeries, thereby decreasing health risks, costs and scarring. Additionally, in contrast to the metals currently utilized, the wear products of which can be potentially toxic or otherwise harmful to the patient [10-13], the corrosion products of Mg have been shown to be potentially beneficial to the patient [14].

The degradable properties of Mg and its alloys are, however, a double-edged sword. Mg is a highly reactive metal, and corrosion rates when immersed in physiological solutions are highand can influence mechanical properties of these alloys also [15-17]. In order for use of this material to be feasible for orthopaedic applications, the corrosion mechanisms must be reduced and controlled. In response to this, coatings have been suggested as a means of reducing exposure to the corrosive environment, thus reducing the corrosion rate. Ideally, corrosion would be slowed to allow the mechanical integrity of the metal to remain intact during bone healing. This would also minimize hydrogen production, which has been observed as a (potentially disadvantageous) corrosion by product when using this material [18–21]. Theoretically, it would be then expected a coating to slowly wear away, allowing controlled degradation of the substrate [22].

Actual research in the field of surface treatments of magnesium alloys is focused on the preparation and evaluation of biocompatible coatings and layers [23, 24]. Biocompatible protective coatings are a practical option to moderate biodegradation allowing functional implant deployment [25, 26].

Especially, coatings with CaP compounds attract attention [27]. Biologically relevant CaP belongs to the orthophosphate group and naturally occurs in several biological structures, including teeth and bone. Consequently, CaP have long been investigated and utilized as coatings for protection against wear corrosion and increased biocompatibility in orthopedic devices [22].

Compared to conventional preparation methods, such as hot spraying or laser cladding, the structure of Ca–P coatings formed in solution is closer to that of the bone minerals [28]. Moreover, the electrodeposition technique could cost-effectively adjust the morphologies and compositions of Ca–P coatings [29].

Thus, the aim of this paper is to find the optimal temperature of CaP electrodeposition process on a surface of the AZ31 magnesium alloy in order to reach the maximal improvement of corrosion properties of the surface.

## 2 Experimental material and methods

The tested AZ31 magnesium alloy was continually casted at Brandenburgische Universität in Cottbus, Germany and chemical composition was analysed at the Magnesium innovation centre MagIC GKSS Geesthacht, Germany. The chemical composition is listed in **Table 1**. The specimens for metallographic observation were prepared by conventional metallographic procedures. For visualization of the magnesium alloy microstructure, etchant consisting of 2.5 ml acetic acid + 2.1 g picric acid + 5 ml $H_2O$ + 35 ml of ethanol was used [30]. The microstructure of AZ31 alloy (**Fig. 1**) was observed by the CARL ZEISS AXIO Imager.A1m light metallographic microscope in the laboratories of Department of Materials Engineering, University of Žilina. The microstructure is created by polyedric grains of supersaturated solid solution of aluminium, zinc and other alloying elements in magnesium. The average grain size is 220 μm.

DOI 10.12776/ams.v20i2.290 p-ISSN 1335-1532
e-ISSN 1338-1156

**Table 1** Chemical composition of AZ31 alloy

| **Component** | Al | Zn | Mn | Si | Cu | Ni | Fe | Mg |
|---|---|---|---|---|---|---|---|---|
| **wt. %** | 2.96 | 0.828 | 0.433 | 0.004 | 0.004 | <0.001 | 0.002 | balance |

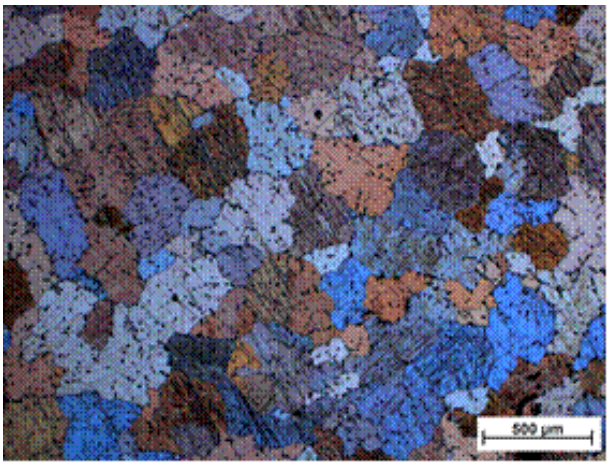


**Fig. 1** Microstructure of AZ31 alloy, light microscopy (polarized light), etch. acetic acid + picric acid + water + ethanol

Before the electrodeposition of calcium phosphate, the specimens were firstly grinded with an emery paper of P1000 to ensure similar surface roughness. Electrodeposition was carried out at 10, 20, 30, 40 and 50 °C for 60 min in a solution of 0.1 M $Ca(NO_3)_2.4H_2O$, 0.06 M $NH_4H_2PO_4$, 10 ml.dm$^{-3}$ of 50 vol.% $H_2O_2$, with a pH of 4 on a laboratory apparatus VSP (producer BioLogic SAS France). The specimens were connected as cathode at controlled potential of -1.8 V vs. saturated calomel reference electrode (SCE). After electrodeposition specimens were immediately rinsed with demineralized water and dried using a stream of air. The evaluation of the deposition process was described in a previous study [31].

The surface morphology of the treated specimens was assessed in the laboratories of the Department of Materials Engineering, FME, University of Žilina, by a stereomicroscope Nikon AZ100 with a digital camera using NIS Elements software. The corrosion characteristics of the untreated and CaP-coated AZ31 after electrodeposition at various temperatures were evaluated by electrochemical impedance spectroscopy (EIS) using a potentiostat/galvanostat/frequency response analyser VSP from BioLogic SAS France. All the corrosion experiments were performed at 22 ± 1 °C in 0.9% NaCl solution simulating the concentration of NaCl in human body environment. A saturated calomel electrode and a platinum electrode served as the reference and auxiliary electrodes, respectively. Treated and untreated AZ31 specimens formed the workingelectrode (a classical three electrode system) in such a way that only 1 cm$^2$ area of the working electrode surface was exposed to the electrolyte solution in corrosion cell. Stabilization time of open circuit potential after immersion of the working electrode into electrolyte was 5 minutes. Measurements were performed at open circuit potential with AC voltage amplitude of 15 mV in frequency range from 100 kHz to 20 mHz. EIS measurements resulted in Nyquist plots that were further analysed by software EC-Lab V10.12 using equivalent circuits shown in **Fig. 2.**

DOI 10.12776/ams.v20i2.290 p-ISSN 1335-1532
e-ISSN 1338-1156

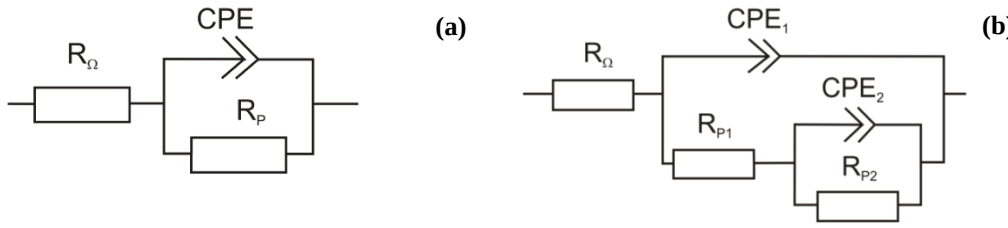


**Fig. 2** Equivalent circuits used for analysis of Nyquist plots: a) For Nyquist plots with one capacitive loop, b) For Nyquist plots with two well-defined capacitive loops

**Fig. 2a** expresses the equivalent circuit used for Nyquist plots with one capacitive loop and **Fig. 2b** the equivalent circuit used for Nyquist plots with two well-defined capacitive loops. These equivalent circuits use various elements expressing the character of evaluated surface. In our case, $R_\Omega$ is resistance of the solution, $R_{p1}$ and $R_{p2}$ are polarization resistances of various mechanisms in corrosion model (e.g. charge transfer, film resistance,...), $R_p$ is mixed polarization resistance or sum of partialpolarisation resistances ($R_{p1} + R_{p2}$) and $CPE_1$ and $CPE_2$ are constant phase elements of mechanisms corresponding with $R_{p1}$ and $R_{p2}$, respectively. $CPE_1$ in second equivalent circuit is constant phase element of the layer of corrosion products.

## 3 Results and discussion

Electrodeposition under specified conditions led to the creation of a thin layer of CaP at all temperatures (**Fig. 3**). The layer of CaP continuously covering the entire surface was composed of irregularly branched units that overlapped each other.

As can be seen, the effect of different temperatures of electrodeposition on the optical features of the surface was not very significant in the temperature range from 10 to 40 °C. By rising temperature of the process only a small increase in CaP crystal units size was observed. This increase was the most significant at 40 and 50 °C, when the formation of a new type of CaP crystals started to appear also.

In **Fig. 4** is listed the time dependence of current densities recorded at VSP laboratory equipment showing behaviour of the electrodeposition process on the surface of the substrate at various temperatures. As can be seen the temperature increase caused shortening of the time, when a maximal current density was reached. This stage of the process represents the situation, when the half of the surface was covered by CaP crystals. It means that the increase of the process temperature accelerated the formation of CaP crystals. Also a sooner beginning of the current density saturation and growth of maximal current density appeared at higher temperature up to 30 °C. All these process changes could be caused by increased diffusion rate of the solution components that is directly related to temperature growth.

Decrease in stability of CaP formation was observed at the temperatures higher than 30 °C. It was represented by the decrease of current density maximum and insufficient or missing current density saturation phase in the final part of the electrodeposition process at 40 and 50 °C. This leaded to the gradual loss of the CaP surface layer quality and isolation properties.

A very important characteristic best describing the resistance of the surface layer (or layers) of the certain material against corrosion is a polarization resistance $R_p$. Its values were obtained by

DOI 10.12776/ams.v20i2.290 p-ISSN 1335-1532
e-ISSN 1338-1156

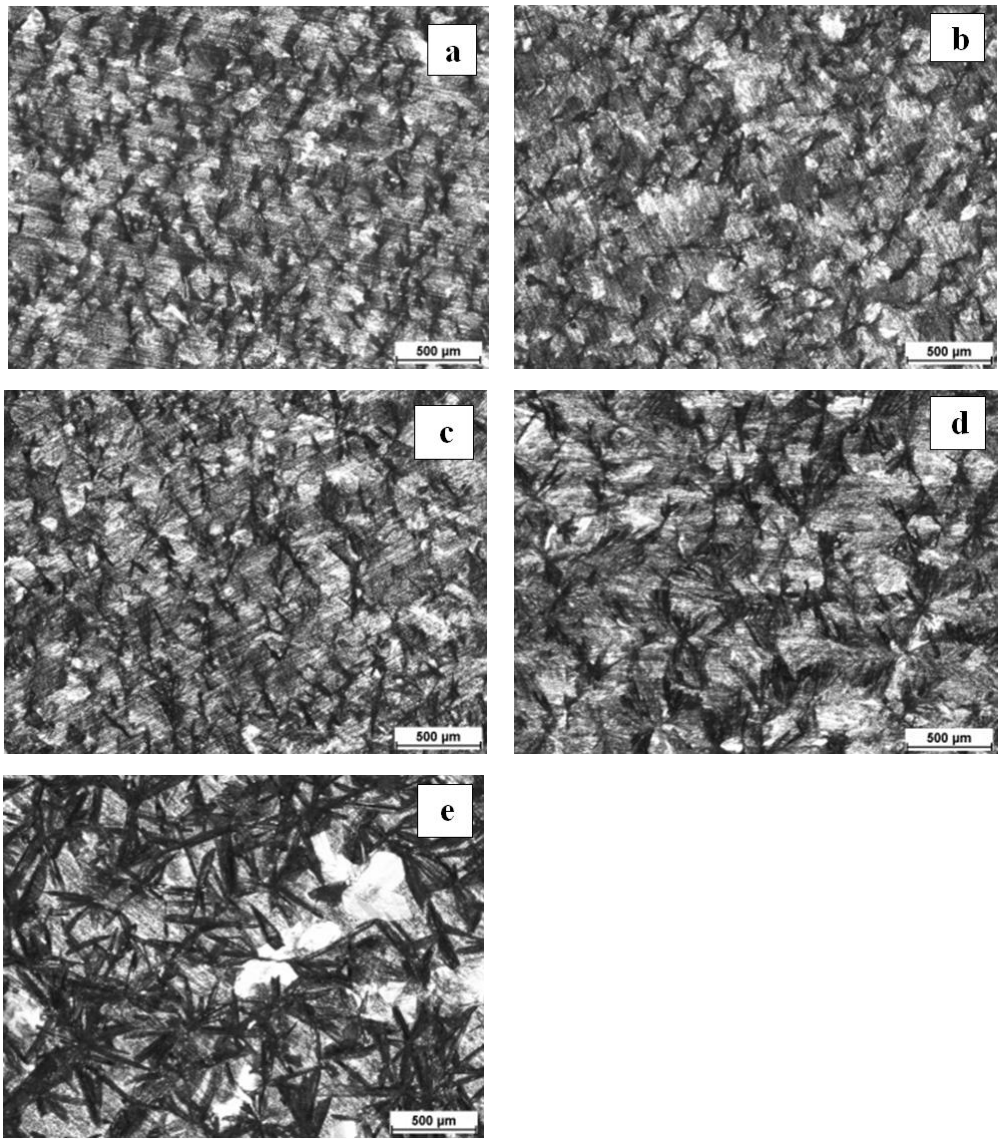


**Fig. 3** Photodocumentation of calcium phosphate surface layer prepared by electrodeposition at various temperatures, light microscopy: a) 10 °C, b) 20 °C, c) 30 °C, d) 40 °C, e) 50 °C

electrochemical impedance spectroscopy, which is one of the non-destructive methods for surface layers examination. By measuring $R_p$ values of CaP surface layer after electrodeposition at various temperatures (**Table 2**), an increase in the corrosion protection was evaluated. As can be seen from Nyquist plots measured on AZ31 surface after electrodeposition at various temperatures (**Fig. 5**) respectively from the diagram showing polarization resistance $R_p$ change (**Fig. 6**), there was an increase of $R_p$ up to maximal value reached after electrodeposition at 30 °C (31981 $\Omega.cm^2$) followed by its gradual decrease. It means that the conditions for the most

DOI 10.12776/ams.v20i2.290 p-ISSN 1335-1532
e-ISSN 1338-1156

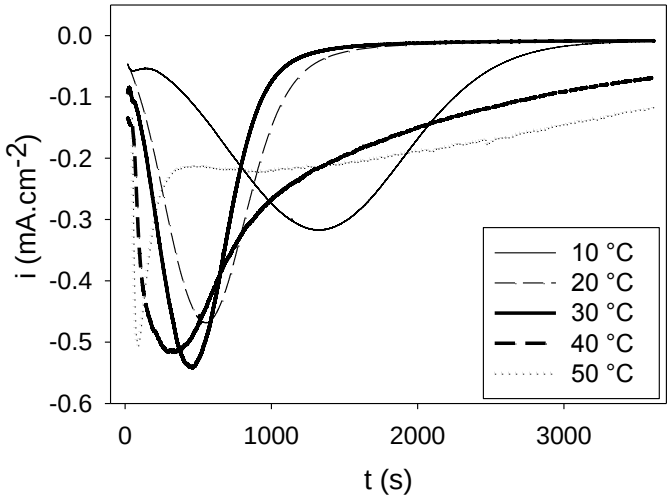


**Fig. 4** Diagram of time dependence of current density during the electrodeposition process of CaP at various temperatures

satisfactory CaP surface layer including diffusion factors and stability of CaP formation were achieved at the range of temperatures near 30 °C. The value of $R_p$ reached after electrodeposition of CaP at 30 °C was 22-fold higher compared to $R_p$ value of non-treated specimens of AZ31 (1403 Ω.cm$^2$). Electrodeposition of CaP at other used temperatures leaded also to the formation of sufficient CaP surface layer with increased corrosion protection compared to non-treated specimens, but the layer was of the lower corrosion resistance quality. This could possibly lead to sooner dissolution of CaP layer and inadequate long-term corrosion protection of the base material.

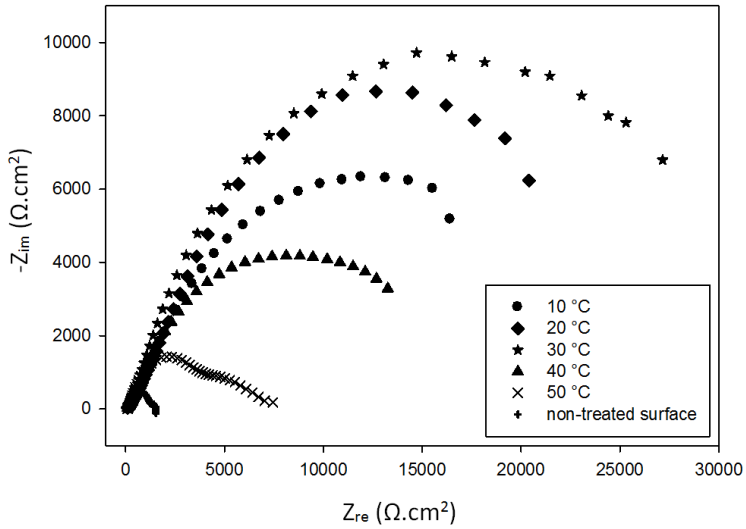


**Fig. 5** Nyquist plots of CaP surface layer on AZ31 alloy after electrodeposition of CaP at various temperatures

DOI 10.12776/ams.v20i2.290 p-ISSN 1335-1532
e-ISSN 1338-1156

**Table 2** Electrochemical characteristics of CaP surface layer on AZ31 alloy surface after electrodeposition of CaP at various temperatures

| | $R_\Omega$ ($\Omega.cm^2$) | $R_{p1}$ ($\Omega.cm^2$) | $R_{p2}$ ($\Omega.cm^2$) | $R_p$ ($\Omega.cm^2$) | $CPE_1$ ($10^{-6}.F.s^{n_1-1}$) | $CPE_2$ ($10^{-6}.F.s^{n_2-1}$) | $n_1$ | $n_2$ |
|---|---|---|---|---|---|---|---|---|
| **non-treated** | 65 | 1157 | 246 | 1403 | 11.3 | 1430.0 | 0.92 | 1 |
| **10 °C** | 48 | 21602 | - | 21602 | 23.2 | - | 0.67 | - |
| **20 °C** | 52 | 25402 | - | 25402 | 18.8 | - | 0.74 | - |
| **30 °C** | 60 | 31981 | - | 31981 | 11.8 | - | 0.71 | - |
| **40 °C** | 64 | 15711 | - | 15711 | 25.1 | - | 0.64 | - |
| **50 °C** | 65 | 1980 | 5251 | 7231 | 14.0 | 159.3 | 0.96 | 0.47 |

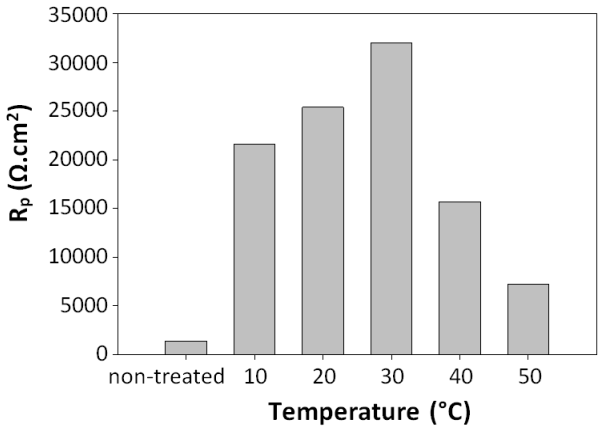


**Fig. 6** Polarization resistance after electrodeposition of CaP at various temperatures

## 4 Conclusions

On the basis of performed experiments, analysis of the results and their interpretations, we concluded the following conclusions:

- Calcium phosphate layer created by electrodeposition at all tested temperatures continuously covers the entire surface of the substrate and is formed by irregular branched units that overlap each other.
- Higher electrodeposition temperature leads to small increase in CaP crystal units' size.
- Rising temperature significantly influences all the stages of CaP electrodeposition process.
- Electrodeposition of CaP at all used temperatures leads to the formation of CaP surface layer increasing corrosion protection of the base material.
- The highest corrosion protection represented by the highest value of $R_p$ and the most advantageous process of electrodeposition was reached after electrodeposition of CaP on AZ31 magnesium alloy surface at temperatures around 30 °C.

## References

[1] M. P. Staiger, A. M. Pietak, J.Huadmai, G. Dias: Biomaterials, Vol. 27, 2006, No. 9, p. 1728–1734, doi:10.1016/j.biomaterials.2005.10.003

DOI 10.12776/ams.v20i2.290 p-ISSN 1335-1532
e-ISSN 1338-1156

[2] M. Niinomi: Metallurgical and Materials Transactions A, Vol. 33, 2002, No. 3, p. 477–486, doi:10.1007/s11661-002-0109-2
[3] J. Nagels, M. Stokdijk, P. M. Rozing: Journal of Shoulder and Elbow Surgery,Vol. 12, 2003, No. 1, p. 35–39, doi:S1058-2746(02)00002-2
[4] J. E. Gray-Munro, C. Seguin, M. Strong: Journal of Biomedical Materials Research A, Vol. 91A, 2009, No. 1, p. 221–230, doi:10.1002/jbm.a.32205
[5] A. Abdal-hay, N. A. M. Barakat, J. K. Lim: Ceramics International, Vol. 39, 2013, p. 183-195, doi:10.1016/j.ceramint.2012.06.008
[6] B. Mordike, T. Ebert: Material Science and. Engineering A, Vol. 302, 2001, No. 1, p. 37–45, doi:10.1016/S0921-5093(00)01351-4
[7] R. C. Zeng, W. Dietzel, F. Witte, N. Hort, C. Blawert: Advanced Engineering Materials, Vol. 10, 2008, No. 8, p. 3-14, doi: 10.1002/adem.200800035
[8] S. Hasegawa, Y. Tsuchida, H. Yano, M. Matsui: International Journal of Fatigue, Vol. 29, 2007, No. 9–11, p. 1839-1845, doi:10.1016/j.ijfatigue.2006.12.003
[9] A. N. Chamos, Sp. G. Pantelakis, G. N. Haidemenopoulos, E. Kamoutsi: Fatigue & Fracture of Engineering Materials & Structures, Vol. 31, 2008, No. 9, p. 812–821, doi:10.1111/j.1460-2695.2008.01267.x
[10] H. Agins, N. Alcock, M. Bansal, E. Salvati, P. Wilson, P. Pellicci: Journal of Bone Joint Surgery, Vol. 70, 1988, No. 3, p. 347-356
[11] V. Langkamer, C. Case, P. Heap, A. Taylor, C. Collins, M. Pearse: Journal of Bone Joint Surgery, Vol. 74, 1992, No. 6, p. 831-838
[12] T. Albrektsson: Critical Reviews in Biocomposition, Vol. 1, 1985, No. 1, p. 53–84
[13] J. Black: Journal of Bone Joint Surgery, Vol. 70, 1988, No. 4, p. 517-519
[14] R.M. Touyz: Frontiers in Bioscience, Vol. 9, 2004, No.1, p. 1278–1293
[15] M. Alvarez-Lopez, M. D. Pereda, J. A. del Valle, M. Fernandez-Lorenzo, M. C. Garcia-Alonso, O. A. Ruano, M. L. Escudero: Acta Biomaterialia, Vol. 6, 2010, No. 5, p. 1763–1771, doi:10.1016/j.actbio.2009.04.041
[16] A. N. Chamos, S.G. Pantelakis, V. Spiliadis: Materials & Design, Vol. 31, 2010, No. 9, p. 4130–4137, doi:10.1016/j.matdes.2010.04.031
[17] P. Doležal, J. Zapletal, M. Horynová, P. Gejdoš, L. Čelko: Chemické listy, Vol. 105, 2011, No. 17, p. 787-789
[18] B. Denkena, A. Lucas: CIRP Annals – Manufacturing Technology, Vol. 56, 2007, No. 1, p. 113–116, doi:10.1016/j.cirp.2007.05.029
[19] B. Zberg, P.J. Uggowitzer, J.F. Löffler: Nature Materials, Vol. 8, 2009, No. 11, p. 887–891, doi: 10.1038/nmat2542
[20] F. Witte, V. Kaese, H. Haferkamp, E. Switzer, A. Meyer-Lindenberg, C.J. Wirth, H. Windhagen: Biomaterials, Vol. 26, 2005, No. 17, p. 3557–3563, doi:10.1016/j.biomaterials.2004.09.049
[21] G. Song, A. Atrens: Advanced Engineering Materials, Vol. 5, 2003, No. 12, p. 837–858, doi: 10.1002/adem.200310405
[22] S. Shadanbaz, G. J. Dias: Acta Biomaterialia, Vol. 8, 2012, p. 20–30, doi:10.1016/j.actbio.2011.10.016
[23] F. Pastorek, B. Hadzima, P. Dolezal: Komunikácie, Vol. 14, 2012, No. 4, p. 26-30
[24] X. B. Chen, D. R. Nisbet, R. W. Li, P. N. Smith, T. B. Abbott, M. A. Easton, D. -H. Zhang, N. Birbilis: ActaBiomaterialia, In Press, 2013, doi:10.1016/j.actbio.2013.11.016

DOI 10.12776/ams.v20i2.290 p-ISSN 1335-1532
e-ISSN 1338-1156

[25] J.E. Gray, B. Luan: Journalof Alloys and Compounds, Vol. 336, 2002, p. 88–113, doi:10.1016/S0925-8388(01)01899-0
[26] X. B. Chen, N. Birbilis, T. B. Abbott: Corrosion Science, Vol. 53, 2011, p. 2263-2268, doi:10.1016/j.corsci.2011.03.008
[27] J. Waterman: Material Science and Engineering B, Vol. 176, 2011, p. 1756-1760, doi:10.1016/j.mseb.2011.06.021
[28] J. M. Zhang, C. J. Lin, Z. D. Feng, Z. W. Tian: Journal of Electroanalytical Chemistry, Vol. 452, 1998, No. 2, p. 235–240, doi:10.1016/S0022-0728(98)00107-7
[29] Y. Song, S. Zhang, J. Li, Ch. Zhao, X. Zhang: Acta Biomaterialia, Vol. 6, 2010, p. 1736-1742, doi:10.1016/j.actbio.2009.12.020
[30] ASM Handbook, Vol. 9: *Metallography and Microstructures*, Ed. G.F. Van der Voort, ASM International, New York, 2004
[31] F. Pastorek, B. Hadzima: Material Engineering – Materiálové Inžinierstvo, Vol. 20, 2013, p. 54-63

**Acknowledgements**

*The research is supported by European regional development fund and Slovak state budget by the project "Research centre of the University of Žilina", ITMS 26220220183 and "Unique equipment for evaluation of tribological properties of machines parts surfaces", ITMS 26220220048. Authors are grateful for the support of experimental works by project VEGA No. 1/0831/13.*